Supporting Information

Mimicry of Sputtered *i*-ZnO Thin Films Using Chemical Bath Deposition for Solution-Processed Solar Cells

Enrico Della Gaspera, [*,†] *Joel van Embden,*[†] *Anthony S. R. Chesman,* [†] *Noel W. Duffy,*[†] *Jacek J. Jasieniak*[*,†]

[†] CSIRO Manufacturing Flagship, Bayview Avenue, Clayton, Victoria 3168, Australia

Corresponding Authors:

enrico.dellagaspera@csiro.au (E.D.G.)

jacek.jasieniak@csiro.au (J.J.J.)

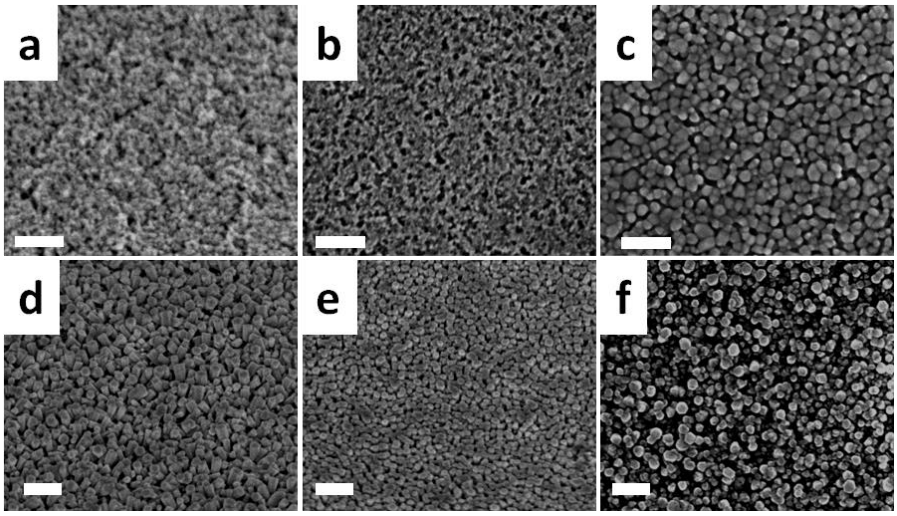

Figure S1. (a-c) SEM micrographs of ZnO seeds: NPs annealed at 180 °C (a), sol-gel annealed at 180 °C (b), sol-gel annealed at 400 °C (c). (d-f) SEM micrographs of ZnO deposited from chemical bath using different seeds: NPs (d), sol-gel annealed at 180 °C (e) and sol-gel annealed at 400 °C (f). Scale bars are 100 nm for panels a-c and 200 nm for panels d-f.

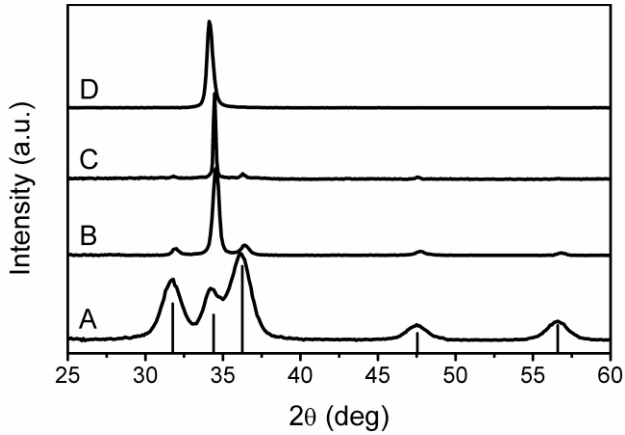

Figure S2. XRD patterns of different ZnO films: (A) deposited from a NPs solution and annealed at 180 °C; (B) deposited from sol-gel and annealed at 400 °C; (C) deposited from chemical bath at 70 °C; (D) sputtered. The reference pattern for wurtzite ZnO is shown at the bottom. The average crystallite size evaluated with the Scherrer formula is about 6 nm, 19 nm, 53 nm and 21 nm for patterns A, B, C and D, respectively.

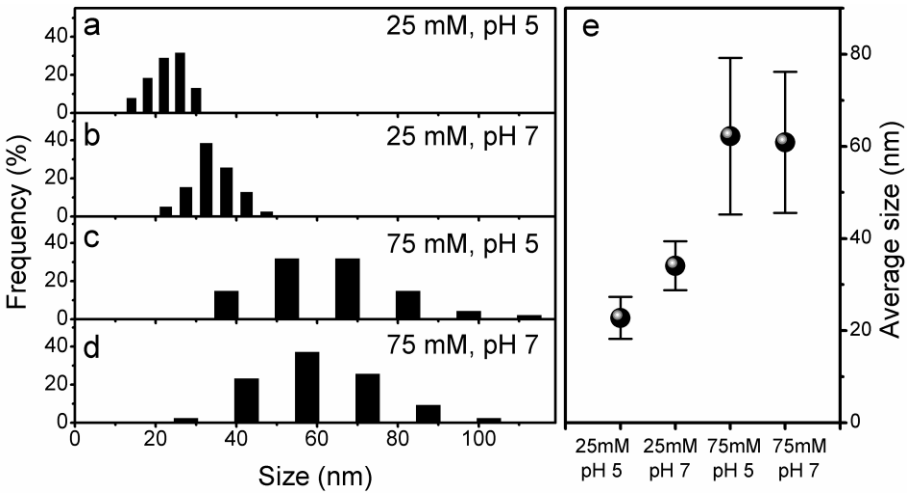

Figure S3. (a-d) Distribution of the lateral size of ZnO grains evaluated from the top view images of Figure 2a. (e) Plot of the average size of the top surfaces of ZnO crystals as a function of the bath conditions. The errors are plus or minus one standard deviation.

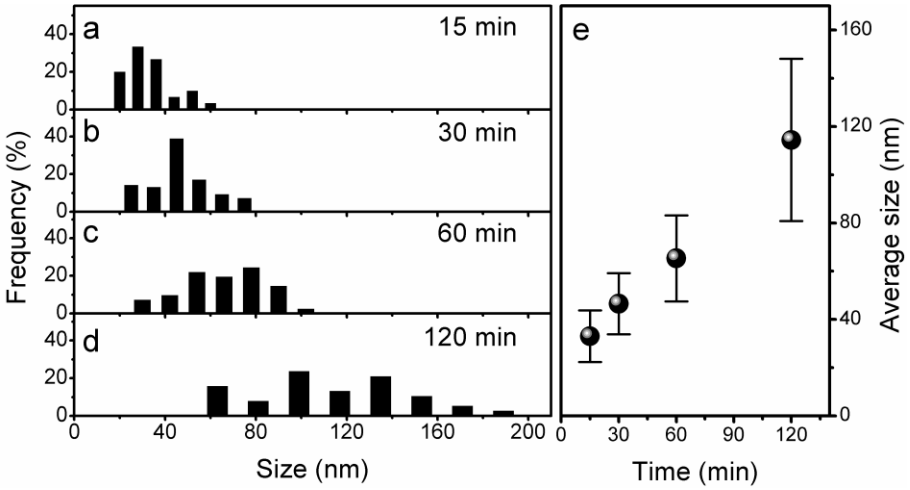

Figure S4. (a-d) Distribution of the lateral size of ZnO grains evaluated from the top view images of Figure 2c. (e) Plot of the average size of the top surfaces of ZnO crystals as a function of the deposition time. The errors are plus or minus one standard deviation.

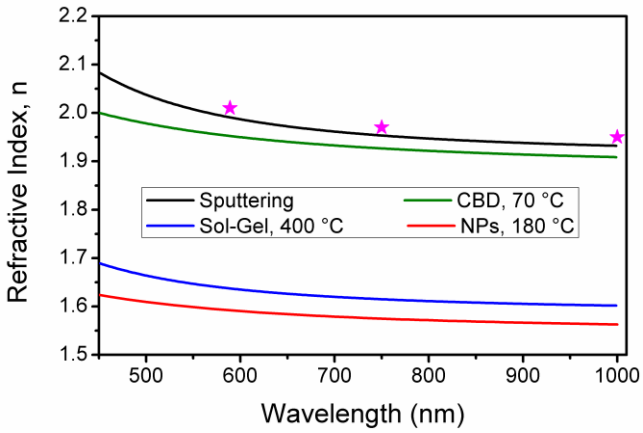

Figure S5. Refractive index dispersion curves for different types of ZnO thin films. The values at three wavelengths for fully dense, bulk ZnO are reported as pink stars.[1]

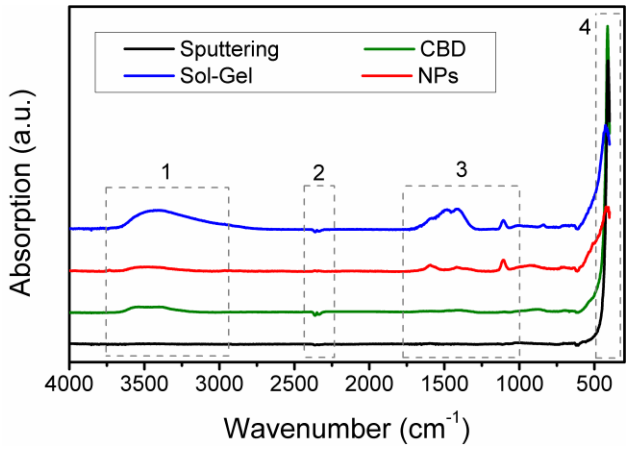

Figure S6. FTIR spectra of different ZnO films. The sputtered film does not show any vibrational peaks beside the one related to ZnO (box 4), while the sol-gel film shows prominent –OH (box 1) and organic (box 3) vibrations. ZnO film from NPs also presents peaks related to organic and hydroxyl groups, even if much weaker compared to the sol-gel film, while the sample prepared from CBD shows a very intense ZnO peak and only a minor contribution from –OH vibrations. The peaks highlighted in box 2 are due to CO_2.

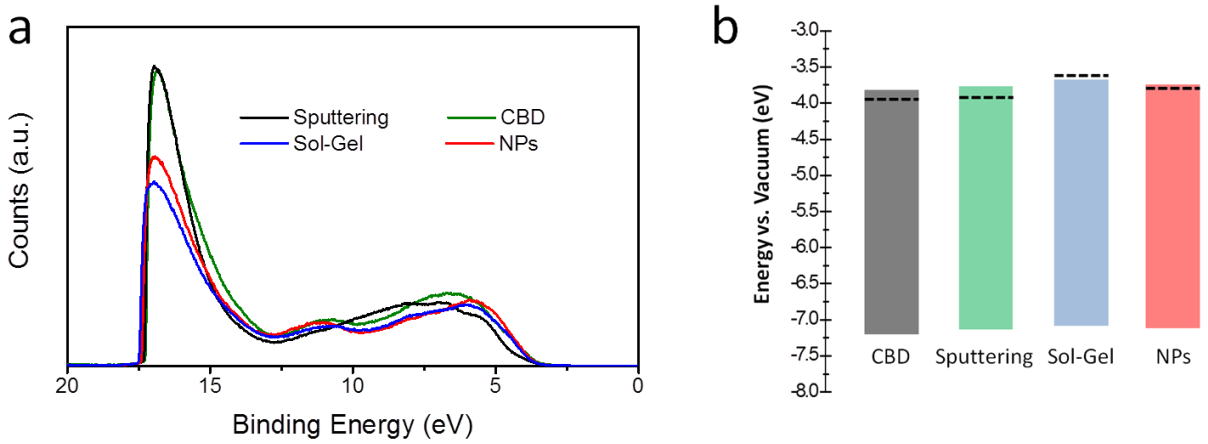

Figure S7. (a) UPS spectra of different ZnO films. (b) Schematic diagram of the flat-band energies derived from UPS data for different ZnO films. The Fermi energies are included as dashed lines. For the actual values, refer to Table S5.

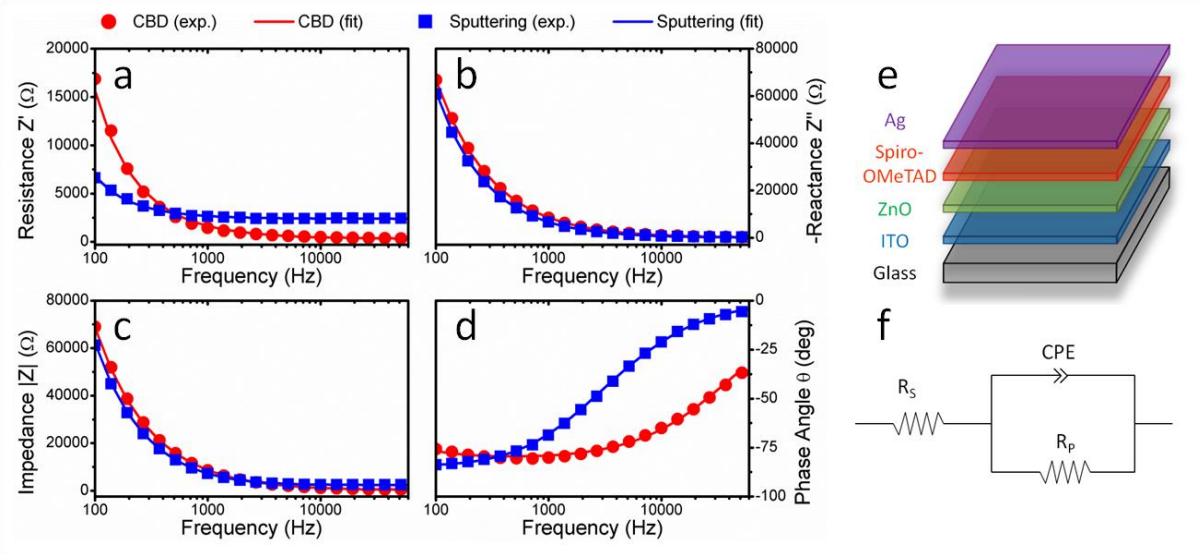

Figure S8. (a) Resistance, (b) reactance, (c) impedance and (d) phase angle plots as a function of frequency for ZnO films prepared via CBD (red dots) and sputtering (blue squares) measured using impedance spectroscopy. The continuous lines are the fits of the experimental data. (e) Schematic representation of the diode architecture. (f) Equivalent circuit diagram used to model the experimental data, where R_S is the series resistance, R_P is the parallel resistance and CPE is the constant phase element (see Table S6 for the modeling results).

Table S1. Optimized conditions for the CBD of thin and dense ZnO films.

Parameter	Investigated conditions	Optimized conditions	Comments
Seed layer	NPs, sol-gel. Annealed up to 400 °C	Sol-gel, annealed at 180 °C	/
Zinc nitrate concentration	25-75 mM	75 mM	Concentration in the final bath.
HMTA concentration	25-75 mM	75 mM	Concentration in the final bath.
pH of starting zinc solution	4-7	7	Adjusted with aqueous NH_3 solution.
Bath temperature	60-90 °C	70 °C	/
Reaction time	Up to 4 hours	30-60 min	Thickness between 100 and 150 nm.
Sample position	Standing vertical, or inclined ±30 deg.	Seeded surface facing down, inclined ~10 deg.	Facing down to avoid precipitates settling on the growing surface.

Table S2. Thickness (t) and average surface roughness (R_a) of the ZnO samples prepared via CBD (refer to Figure 2c for SEM characterization) and sputtering (refer to Figure 3 for SEM characterization) as measured with profilometry.

Sample	t (nm)	R_a (nm)
CBD 15 min	65	1.6±1.1
CBD 30 min	100	1.4±0.3
CBD 60 min	140	2.6±1.3
CBD 120 min	295	4.9±3.7
Sputtering	150	2.1±1.8

Table S3. Relative intensities of five different diffraction peaks, texture coefficient *P* along the (002) direction and alignment factor *A* for different ZnO films evaluated from the XRD patterns of Figure S2.

	$I_{(100)}$	$I_{(002)}$	$I_{(101)}$	$I_{(102)}$	$I_{(110)}$	$P_{(002)}$	A (%)
Ref. (ICDD No. 36-1451)	57	44	100	23	32	1	0
Sputtered	0	100	0	0	0	5	100
CBD	2	100	4.5	2.3	0.8	4.60	90
Sol-Gel at 400 °C	7.9	100	12	4.6	3.2	4.01	75
NPs at 180 °C	70	59	100	19	22	1.29	7

The texture coefficient *P* of the (*hkl*) diffraction is calculated according to the formula:

$$\boldsymbol{P}\,(\boldsymbol{h_i k_i l_i}) = \frac{\boldsymbol{I}\,(\boldsymbol{h_i k_i l_i})}{\boldsymbol{I_0}(\boldsymbol{h_i k_i l_i})}\left[\frac{\boldsymbol{1}}{\boldsymbol{n}}\sum_{\boldsymbol{i=1}}^{\boldsymbol{n}}\frac{\boldsymbol{I}(\boldsymbol{h_i k_i l_i})}{\boldsymbol{I_0}(\boldsymbol{h_i k_i l_i})}\right]^{\boldsymbol{-1}}$$

Where I_0 is the standard intensity, I is the experimental intensity of the $(h_i\, k_i\, l_i)$ diffraction and n is the number of peaks taken into consideration.[2] The texture coefficient ranges between 1 (no alignment) and n (perfect alignment).

We defined the alignment factor *A* as the following:

$$\boldsymbol{A}\,(\%) = \frac{\boldsymbol{P-1}}{\boldsymbol{n-1}} \times \boldsymbol{100}$$

The alignment factor ranges from 0% (no alignment) to 100% (complete alignment).

Table S4. Refractive index values at three different wavelengths for the thin films presented in Figure S6, and relative pores volume fraction evaluated with the Bruggeman relationship.[3]

Sample	$n_{(589\ nm)}$	Porosity (%)	$n_{(750\ nm)}$	Porosity (%)	$n_{(1000\ nm)}$	Porosity (%)
Reference[3]	2.01	/	1.97	/	1.95	/
CBD	1.95	6	1.93	4	1.91	4
Sputtering	1.99	2	1.95	2	1.93	2
Sol-Gel	1.64	35	1.62	34	1.60	35
NPs	1.59	40	1.57	39	1.56	39

Table S5. Valence band (E_{VB}), conduction band (E_{CB}) and Fermi energy (E_f) values for different ZnO films as obtained from UPS. The values for the optical and electrical band gap ($E_{g,op}$ and $E_{g,el}$ respectively) are included as well. The electrical band gap is calculated as the sum of the optical bandgap, derived from optical absorption measurements, and the bulk exciton binding energy (60 meV for ZnO).

Sample	E_{VB} vs. vacuum (eV)	E_f vs. vacuum (eV)	$E_{g,op}$ (eV)	$E_{g,el}$ (eV)	E_{CB} vs. vacuum (eV)
CBD	-7.22	-3.95	3.3	3.36	-3.86
Sputtering	-7.16	-3.92	3.3	3.36	-3.8
Sol-Gel	-7.1	-3.62	3.37	3.43	-3.67
NPs	-7.14	-3.8	3.38	3.44	-3.76

Table S6. Coefficient of determination of the fitting (R^2), series resistance (R_S), parallel resistance (R_P), parallel capacitance (C_P) and exponent of the CPE element (α) for diodes prepared using sputtered and CBD-grown ZnO films as evaluated from impedance spectroscopy measurements. The device prepared without ZnO showed a purely resistive behavior with a resistance of ~30 Ω.

Sample	R^2	R_S (Ω)	R_P (Ω)	C_P (F)	α
CBD	0.945	321	8.52×10^{5}	4.15×10^{-8}	0.91
Sputtering	0.974	2395	1.98×10^{6}	3.02×10^{-8}	0.97

References

(1) Lide, D. R. CRC *Handbook of Chemistry and Physics*, 87th ed; Taylor and Francis: Boca Raton, FL, USA, 2007, 10-248.

(2) Barret, C.; Massalski, T. B. *Structure of Metals*; Pergamon Press: Oxford, UK 1980, 1923.

(3) Bruggeman, D. A. G. Berechnung Verschiedener Physikalischer Konstanten von Heterogenen Substanzen. *Ann. Phys.* (Leipzig, Germany) **1935**, *24*, 636-679.